MATERIALS CHARACTERIZATION 61 (2010) 851–858

available at www.sciencedirect.com

ScienceDirect

www.elsevier.com/locate/matchar

Structure and mechanical properties of as-cast Ti–5Nb–xFe alloys

Hsueh-Chuan Hsu[a,b], Shih-Kuang Hsu[a,b], Shih-Ching Wu[a,b], Chih-Jhan Lee[c], Wen-Fu Ho[c,*]

[a] *Department of Dental Laboratory Technology, Central Taiwan University of Science and Technology, Taichung 40605, Taiwan, ROC*
[b] *Institute of Biomedical Engineering and Material Science, Central Taiwan University of Science and Technology, Changhua 51591, Taiwan, ROC*
[c] *Department of Materials Science and Engineering, Da-Yeh University, Changhua 51591, Taiwan, ROC*

ARTICLE DATA

Article history:
Received 1 December 2009
Received in revised form 5 May 2010
Accepted 5 May 2010

Keywords:
Titanium alloys
Mechanical properties
Phase transformation

ABSTRACT

In this study, as-cast Ti–5Nb and a series of Ti–5Nb–*x*Fe alloys were investigated and compared with commercially pure titanium (c.p. Ti) in order to determine their structure and mechanical properties. The series of Ti–5Nb–*x*Fe alloys contained an iron content ranging from 1 to 5 mass% and were prepared by using a commercial arc-melting vacuum-pressure casting system. Additionally, X-ray diffraction (XRD) for phase analysis was conducted with a diffractometer, and three-point bending tests were performed to evaluate the mechanical properties of all specimens. The fractured surfaces were observed by using scanning electron microscopy (SEM). The experimental results indicated that these alloys possessed a range of different structures and mechanical properties dependent upon the various additions of Fe. With an addition of 1 mass% Fe, retention of the metastable β phase began. However, when 4 mass% Fe or greater was added, the β phase was entirely retained with a bcc crystal structure. Moreover, the ω phase was only detected in the Ti–5Nb–2Fe, Ti–5Nb–3Fe and Ti–5Nb–4Fe alloys. The largest quantity of ω phase and the highest bending modulus were found in the Ti–5Nb–3Fe alloy. The Ti–5Nb–2Fe alloy had the lowest bending modulus, which was lower than that of c.p. Ti by 20%. This alloy exhibited the highest bending strength/modulus ratio of 26.7, which was higher than that of c.p. Ti by 214%, and of the Ti–5Nb alloy (14.4) by 85%. Additionally, the elastically recoverable angles of the ductile Ti–5Nb–1Fe (19.9°) and Ti–5Nb–5Fe (29.5°) alloys were greater than that of c.p. Ti (2.7°) by as much as 637% and 993%, respectively. Furthermore, the preliminary cell culturing results revealed that the Ti–5Nb–*x*Fe alloys were not only biocompatible, but also supported cell attachment.

1. Introduction

In comparison with other metallic biomaterials, titanium and titanium alloys are more biocompatible, more corrosion resistant, lighter, more durable, and possess a reasonable balance of high strength and low elastic modulus. For these reasons, titanium and its various alloys are the metals of choice for the manufacture of load-bearing dental and orthopedic implants [1]. Commercially pure titanium (c.p. Ti) has established a reputation for its prosthetic dental applications because of its excellent biocompatibility as a dental metal [2–4]. However, when a higher strength than that

* *Corresponding author*. Tel.: +886 4 8511888ext4108; fax: +886 4 8511280.
E-mail address: fujii@mail.dyu.edu.tw (W.-F. Ho).

1044-5803/$ – see front matter © 2010 Elsevier Inc. All rights reserved.
doi:10.1016/j.matchar.2010.05.003

provided by c.p. Ti is needed, c.p. Ti is enhanced through alloying, which exhibits a solid-solution hardening, lower fusion temperatures and better ductility than c.p. Ti itself [5].

Titanium can be alloyed with a variety of elements to alter its properties and enhance its strength, high temperature performance, creep resistance, weldability and formability [2]. In addition to the aforementioned properties, biocompatibility is also important so that the metal prosthetic does not induce harmful toxicological or allergic reactions in the patient. Ti–6Al–4 V is the most common titanium alloy for surgically implanted parts such as knees, hips and shoulder replacements [6,7]. However, the element V has been found to have severe reactions with animal tissue. Additionally, clinical concerns have been raised that Al may be connected to neurological disorders and Alzheimer's disease [8]. Therefore, Al, V-free titanium alloys, such as Ti–11.5Mo–6Zr–2Fe [4], Ti–29Nb–13Ta–4.6Zr [9], Ti–24Nb–4Zr–7.9Sn [10], Ti–7.5Mo [11,12], Ti–Cr [13] and Ti–Zr [14] have been developed in response to such toxic concerns.

Whereas an implant with a low elastic modulus shares a common load with the bone to facilitate growth, a significant difference in stiffness between implants and bone tissue can lead to a stress-shielding effect, thereby causing possible osteoporosis or poor osseointegration [15,16]. Finite element analysis has shown that a lower modulus hip prosthesis better simulates the natural femur in distributing stress to the adjacent bone tissue [17,18]. Animal studies have also indicated that the bone remodeling commonly performed on hip prosthesis patients may be reduced by a prosthesis having a lower modulus [19,20]. The relatively low moduli of β titanium alloys help to reduce the "stress-shielding" effect [17,21] and have drawn much attention from researchers in this field [4,22].

Ti–Nb based alloys that contain non-toxic elements have now attracted extensive fundamental medical research attention due to their low elastic modulus and shape memory behaviors, as well as their superelasticity [1,18]. By either modifying the available titanium alloys or exploring new compositions, one can achieve better performance through enhancing their biomedical and mechanical properties or workability [23]. For instance, mechanical properties, shape memory behaviors and superelasticity can be further improved upon by the addition of alloy elements, such as Sn [24,25], Zr [26], and Al [27] to the binary Ti–Nb alloys. In this present study, Fe was selected on the basis of its low cost as well as being one of the strongest β phase stabilizers, whose influence has previously been demonstrated on the properties of other titanium systems [28–30]. Consequently, the effects of Fe on the structure and mechanical properties of a Ti–5Nb based alloy are investigated in order to gauge the potential of new alloys for practical biomedical applications.

2. Materials and methods

The materials used for this study include c.p. Ti, Ti–5Nb, Ti–5Nb–xFe (x = 1, 2, 3, 4 and 5 mass%) alloys. All the materials were prepared from raw titanium (ASTM grade 2), niobium (99.95% pure), and iron (99.95% pure) by using a commercial arc-melting vacuum-pressure-type casting system (Castmatic, Iwatani Corp., Japan). Ingots weighing approximately 20 g each were re-melted five times to improve their chemical homogeneity. Prior to casting, the ingots were again re-melted. The difference in pressure between the two chambers allowed the molten alloys to instantly drop into a graphite mold at room temperature. The dimensions of the cast specimens were $40 \times 5 \times 1$ mm^3. The cast alloys were sectioned by using a Buehler Isomet low-speed diamond saw to obtain specimens for various purposes. Surfaces of the alloys for this microstructural study were mechanically polished via a standard metallographic procedure to a final level of 0.3 μm alumina powder. X-ray diffraction for phase analysis was conducted by using a diffractometer (XRD-6000, Shimadzu, Japan) operating at 30 kV and 30 mA. Ni-filtered CuKα radiation was used for this study.

Three-point bending tests were performed by using a desktop mechanical tester (AG-IS, Shimadzu, Japan). The bending strengths were determined by using the equation, $\sigma = 3PL/2bh^2$ [31], where σ is the bending strength (MPa); P, the load (N); L, the span length (mm); b, the specimen width (mm); and h the specimen thickness (mm). The dimensions of the specimens were $L = 30$ mm, $b = 5.0$ mm and $h = 1.0$ mm. The elastic bending modulus was calculated from the load increment and the corresponding deflection increment between the furthest possible on a straight line, using the equation $E = L^3\Delta P/4bh^3\Delta\delta$, where E is the elastic bending modulus (GPa); ΔP, the load increment as measured from the preload (N); and $\Delta\delta$, the deflection increment at midspan as measured from the preload. The average bending strength and modulus of elasticity in bending were obtained from at least five tests under each condition. The elastic recovery (springback) capability for each material was evaluated from the change in the deflection angle when loading was removed. These details have previously been reported by Ho et al. [11]. After the bending test, the fractured surface of the specimen was cleaned by an ultra-sonic washer. This surface was then observed by using scanning electron microscopy (JSM-6700F, JEOL, Japan).

First, cast specimens were mechanically polished to a mirror finish for biocompatibility test. All cast specimens were sterilized in 70% ethanol. Five specimens of each metal were evaluated by the morphology of cell attachment and MTT assay. MG-63 osteoblast-like cells were cultured in Dulbecco's Modified Eagle Medium containing 10% fetal bovine serum, 1% penicillin/strepmycin, 1% L-glutamine and 1% non-essential amino acids in an incubator containing 95% air and 5% CO_2 at 37 °C. The cells were cultured and placed at a density of 1×10^4 cells/ml in direct contact with the specimens. After they were co-cultured for 4 days, the specimens were fixed in a 4% formaldehyde solution for 48 h and dehydrated in increasing ethanol concentrations (30–100%). Finally, the surfaces of the culture specimens were gold-sputtered and examined by scanning electron microscopy. Effect of each alloy on the proliferation of MG-63 cell was investigated by MTT assay. After the incubation, 10 μl of MTT reagent of 5 mg/ml was added, followed by 4-h incubation. The medium was then removed and the wells were washed twice with PBS. Then, 100 μl of DMSO was added in to solubilize the formazan crystals and the optical density (OD) was measured at 550 nm in an ELISA reader (VersaMax, Molecular Device, USA).

3. Results and discussion

3.1. Phase identification

The XRD patterns of Ti–5Nb and the series of ternary Ti–5Nb–*x*Fe alloys are shown in Fig. 1. The crystal structures of the ternary Ti–5Nb–*x*Fe alloys are sensitive to their Fe contents. The Ti–5Nb alloy was comprised mainly of the α′ phase. When 1 or 2 mass% Fe was added, a small amount of the β phase was retained because the alloying element Fe is known to act as a β stabilizer. When the Fe content was increased to 3 mass%, the formation of the α′ phase was largely suppressed whereas the β phase in its high temperature bcc structure was almost entirely retained. When the Fe content was increased to 4 mass% or greater, only the retained β phase was observed in the XRD patterns. This indicated that a more extensive increase in the solute β stabilizing content, under a significant cooling rate from high temperature β field to room temperature, obtained a metastable or even stable β phase.

The presence of an ω phase could be easily detected at a lower scanning speed (0.5°/min), as shown in Fig. 2. The ω phase was only found in the Ti–5Nb–2Fe, Ti–5Nb–3Fe and Ti–5Nb–4Fe alloys, being especially notable in the Ti–5Nb–3Fe and Ti–5Nb–4Fe alloys. For higher Fe contents, the ω phase was no longer observed. Other research has shown that the ω phase occurs in certain titanium based alloys in which the β phase can be retained in a metastable state [32]. According to Sikka et al. [33], this ω phase may be defined by a hexagonal lattice. In many investigations, the presence and relative amount of an ω phase in Ti and Zr alloys can be observed from the intensity of lines on the X-ray diffraction patterns of either polycrystals or through one of the ω phase reflections in photographs of single crystals [32,34,35]. The presence of this athermal ω phase, although small in quantity, has an exceedingly important effect on the mechanical properties of the alloy, as will be discussed later. Afonso et al. [36] also stated that depending on the composition, the ω phase can precipitate within the β matrix, turning the material fragile.

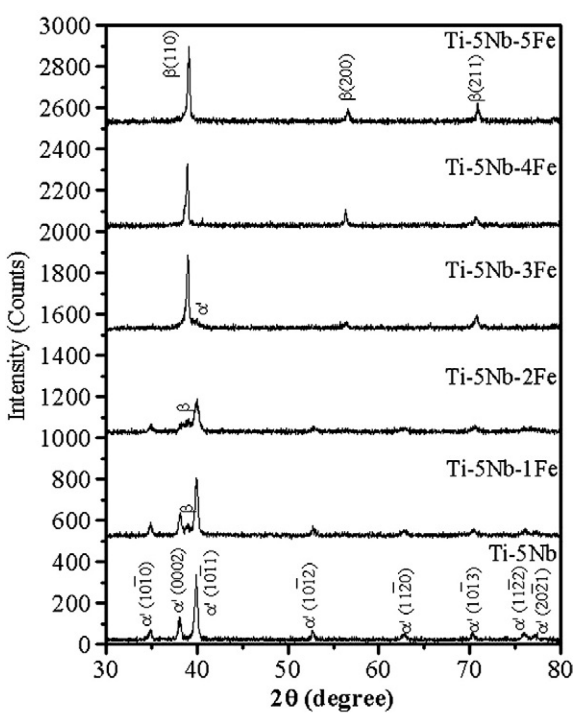

Fig. 1 – XRD patterns of Ti–5Nb and Ti–5Nb–*x*Fe alloys.

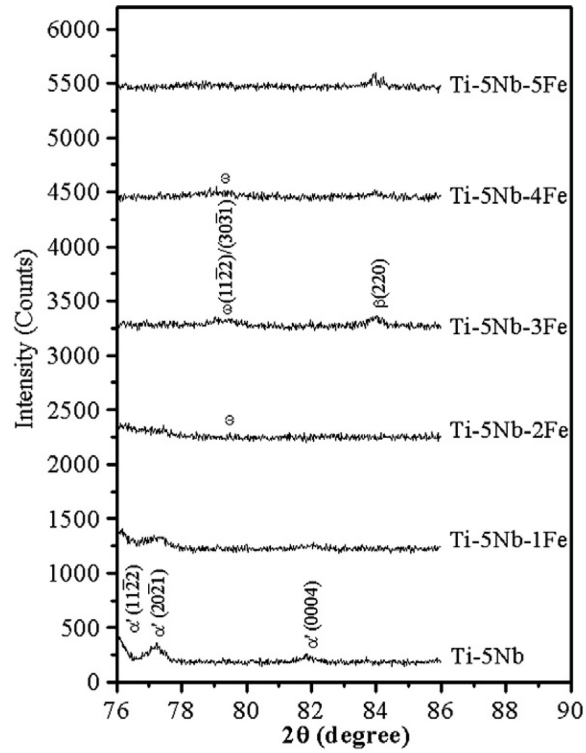

Fig. 2 – Low scanning speed XRD patterns of Ti–5Nb and Ti–5Nb–*x*Fe alloys.

3.2. Mechanical properties

The bending strengths of c.p. Ti, Ti–5Nb and Ti–5Nb–*x*Fe alloys are shown in Fig. 3. All the Ti–5Nb and Ti–5Nb–*x*Fe alloys had

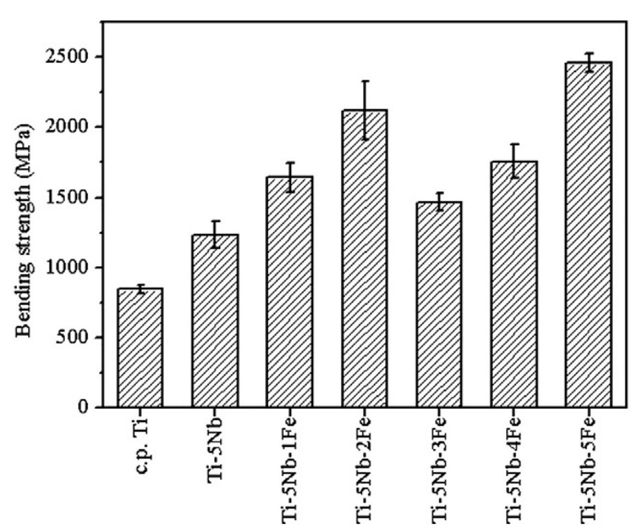

Fig. 3 – Bending strengths of c.p. Ti, Ti–5Nb and Ti–5Nb–*x*Fe alloys.

significantly higher ($p<0.05$) bending strengths (1466–2460 MPa) than the c.p. Ti (844 MPa) tested. Moreover, all the Ti–5Nb–xFe had higher bending strengths than the Ti–5Nb. The Ti–5Nb–2Fe and Ti–5Nb–5Fe alloys had significantly ($p<0.05$) higher bending strengths than the other Ti–5Nb–xFe and Ti–5Nb alloys. It is noteworthy that the bending strengths of the Ti–5Nb–2Fe and Ti–5Nb–5Fe alloys were approximately 2.5 and 2.9 times greater, respectively, than for c.p. Ti. One can conclude that, in this present study, these strengths likely increased due to a solid-solution strengthening effect for higher Fe contents or by the strong hardening effect of the ω phase.

The elastic modulus results are shown in Fig. 4. The Ti–5Nb–3Fe (137 GPa) and Ti–5Nb–4Fe (125 GPa) alloys had significantly higher ($p<0.05$) bending moduli than the c.p. Ti (99 GPa), Ti–5Nb (102 GPa), Ti–5Nb–1Fe (98 GPa), Ti–5Nb–2Fe (79 GPa) and Ti–5Nb–5Fe (104 GPa). ANOVA test results indicated that there are no significant differences among the bending moduli of c.p. Ti, Ti–5Nb, Ti–5Nb–1Fe and Ti–5Nb–5Fe ($p>0.05$). Overall, the Ti–5Nb–3Fe alloy had the highest bending moduli. This result may be associated with the formation of the ω phase during quenching. In this study, the ω phase was observed in the Ti–5Nb–2Fe, Ti–5Nb–3Fe and Ti–5Nb–4Fe alloys, being especially notable in the Ti–5Nb–3Fe and Ti–5Nb–4Fe alloys. The early work of Graft and Rostoker [37] indicated that the ω phase has an unusually high elastic modulus. It is noteworthy that the Ti–5Nb–2Fe alloy had the lowest bending modulus, lower than that of c.p. Ti by 20%. As mentioned in the Introduction, using implant materials with lower moduli (closer to that of a human bone) can reduce the stress-shielding effect. In a study by Ho et al. [29], a bending strength/modulus ratio (×1000) was used to evaluate an indication of feasibility for use as an implant material. In this study, the Ti–5Nb–2Fe alloy exhibited the highest bending strength/modulus ratios of as large as 26.7, being higher than that of c.p. Ti (8.5) by 214%, and of the Ti–5Nb alloy (14.4) by 85%. The high strength/modulus ratios of the Ti–5Nb–2Fe alloy demonstrate its advantage for use as an implant material.

The typical bending stress-deflection profiles of the series of alloys and c.p. Ti are shown in Fig. 5. Although the Ti–5Nb–2Fe, Ti–5Nb–3Fe and Ti–5Nb–4Fe alloys with ω phases failed in brittleness tests (having an average deflection of about 4.9, 1.9 and 2.3 mm, respectively), the Ti–5Nb, Ti–5Nb–1Fe and Ti–5Nb–5Fe alloys without ω phases did not fail, even after being deflected by 8 mm (the pre-set maximum). This ω phase-induced embrittlement was also observed in other Ti alloy systems such as Ti–V [38] and Ti–Mn [39] as early as the 1970s. Recently, Cheng et al. also reported on the mechanical behavior of the ω phase in a Ti–10Zr–xCr alloy system [40]. It is interesting to note that, despite the strong hardening effect of the ω phase, the bending strength of Ti–5Nb–3Fe, the alloy comprising the largest amount of the ω phase, was lower than the alloys containing no ω phase (Ti–5Nb, Ti–5Nb–1Fe and Ti–5Nb–5Fe). This result is attributable to the premature, brittle fracture that occurred in the Ti–5Nb–3Fe alloy. This finding is also consistent with the early results of Koike et al. [41], who examined the characteristics of as-cast Ti–Cr(7–19 mass%)–Cu (3–7 mass%) alloys to evaluate their suitability for dental applications. Those researchers proposed that the elongation of the alloys was dependent on their respective microstructures and chemical compositions. In their studies, the extreme brittleness of the Ti–7Cr alloys was attributed to the presence of the ω phase. Similar results have also been discussed concerning Ti–5Cr–0.5Fe, Ti–5Cr–1Fe and Ti–10Zr–5Cr alloys [29,40].

In this study, only the Ti–5Nb, Ti–5Nb–1Fe and Ti–5Nb–5Fe exhibited ductile properties. It is noteworthy that the advantage of the mechanical properties of the Ti–5Nb–1Fe and Ti–5Nb–5Fe alloys is also demonstrated in their high elastic recovery capability (springback), as shown in Fig. 6. The elastically recoverable angles of the Ti–5Nb–1Fe (19.9°) and Ti–5Nb–5Fe (29.5°) alloys were greater than that of c.p. Ti (2.7°) by as much as 637% and 993%, respectively. This is significant because the high elastic recovery of a metal is essential in many load-bearing implant and dental applications.

3.3. SEM photography

The effect of the ω phase can also be observed in fractography of the alloys. Fig. 7(a)–(c) shows SEM micrographs of the fractured surfaces of the Ti–5Nb–2Fe, Ti–5Nb–3Fe and Ti–5Nb–

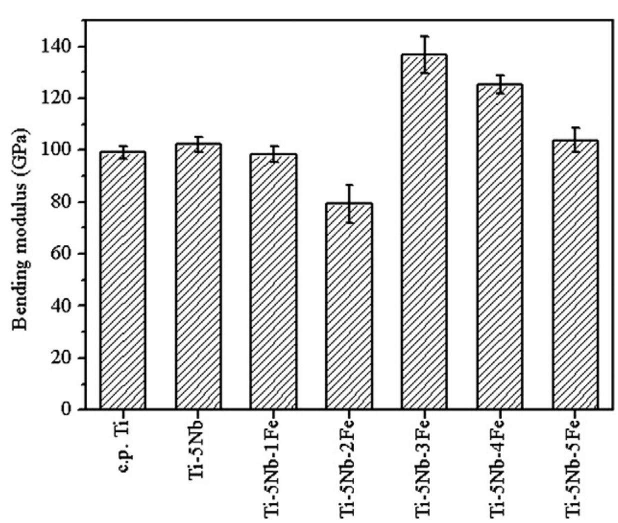

Fig. 4 – Bending moduli of c.p. Ti, Ti–5Nb and Ti–5Nb–xFe alloys.

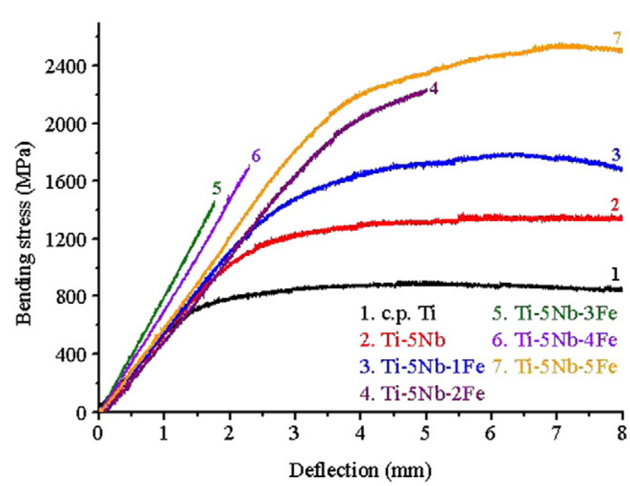

Fig. 5 – Bending stress-deflection profiles of c.p. Ti, Ti–5Nb and Ti–5Nb–xFe alloys.

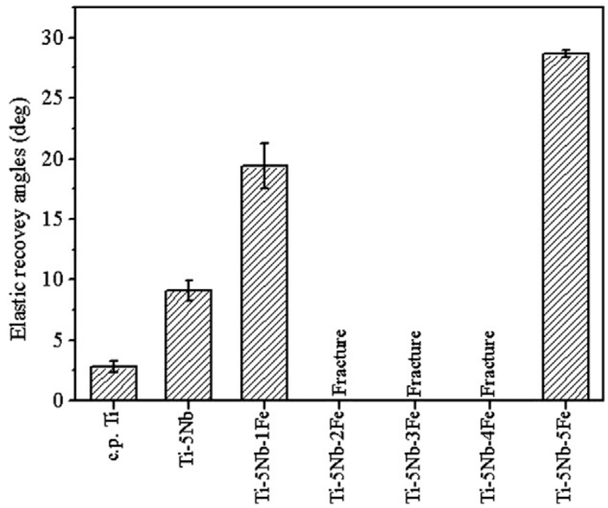

Fig. 6 – Elastic recovery angles of c.p. Ti, Ti–5Nb and Ti–5Nb–xFe alloys.

4Fe specimens after bending tests. Since the Ti–5Nb, Ti–5Nb–1Fe and Ti–5Nb–5Fe alloys did not fail during a bending test, their micrographs were not examined. The Ti–5Nb–3Fe and Ti–5Nb–4Fe alloys were characterized by cleavage facets in the fractured surface, being characteristic of decreased ductility, together with some terrace-type morphology. The cleavage fracture corresponds to the highly brittle feature of these specimens indicated by the extremely low value of the bending deflection (less than approximately 2.3 mm). As shown in Fig. 7(a), the fractured structures of the Ti–5Nb–2Fe alloy exhibited mainly dimple ruptures, indicative of a typical ductile fracture. The dimple nature of the fracture seen in this fractograph is consistent with a fracture deflection of 4.9 mm exhibited by this specimen, being larger than those of the Ti–5Nb–3Fe and Ti–5Nb–4Fe alloys.

3.4. *Cell morphology and MTT assay*

SEM was also used to closely inspect the cell morphology on the as-cast c.p. Ti, Ti–5Nb and Ti–5Nb–*x*Fe alloys. As observed in Fig. 8, osteoblasts extended the pseudopodia and attached onto the substrates for each metal after culturing for 4 days. MTT is a pale yellow substrate that is cleaved in active mitochondria, and the reaction occurs only in living cells. Fig. 9 shows the numbers of MG-63 cells on all samples increased with the incubation time. After culturing for 4 days, the cell proliferated favorably on the Ti–5Nb–*x*Fe alloys. On Ti–5Nb–*x*Fe specimens the proliferation level was slightly higher than on the c.p. Ti, Ti–5Nb and Ti–6Al–4 V. From above result revealed that the as-cast Ti–5Nb and Ti–5Nb–*x*Fe alloys were biocompatible, supporting both the cell attachment and viability.

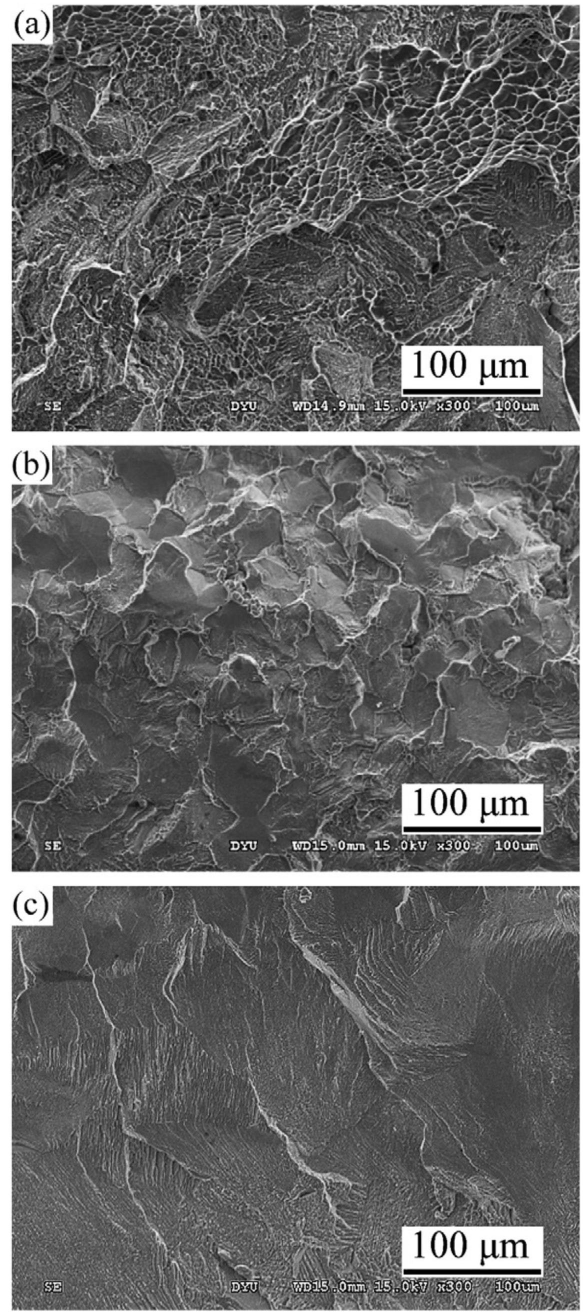

Fig. 7 – SEM fractographs of Ti–5Nb–2Fe (a), Ti–5Nb–3Fe (b) and Ti–5Nb–4Fe (c) alloys at 300× magnification.

4. Conclusions

(1) The Ti–5Nb alloy was comprised mainly of the α' phase. When 1 or 2 mass% Fe was introduced into this alloy, a small amount of β phase was retained. With the addition of 3 mass% Fe, a large amount of the metastable β phase was retained. However, when the Fe content was increased to 4 mass% or greater, the β phase was completely retained with a bcc crystal structure. Moreover, the ω phase was detected in the Ti–5Nb–2Fe, Ti–5Nb–3Fe and Ti–5Nb–4Fe alloys, being especially notable in the Ti–5Nb–3Fe and Ti–5Nb–4Fe alloys.

(2) All the Ti–5Nb and Ti–5Nb–*x*Fe alloys had higher bending strengths (1466–2460 MPa) than c.p. Ti (844 MPa). Additionally, the bending strengths of the Ti–5Nb–2Fe and Ti–5Nb–5Fe alloys were higher than those of the other Ti–5Nbr–*x*Fe and Ti–5Nb alloys. Moreover, the bending strengths for the Ti–5Nb–2Fe

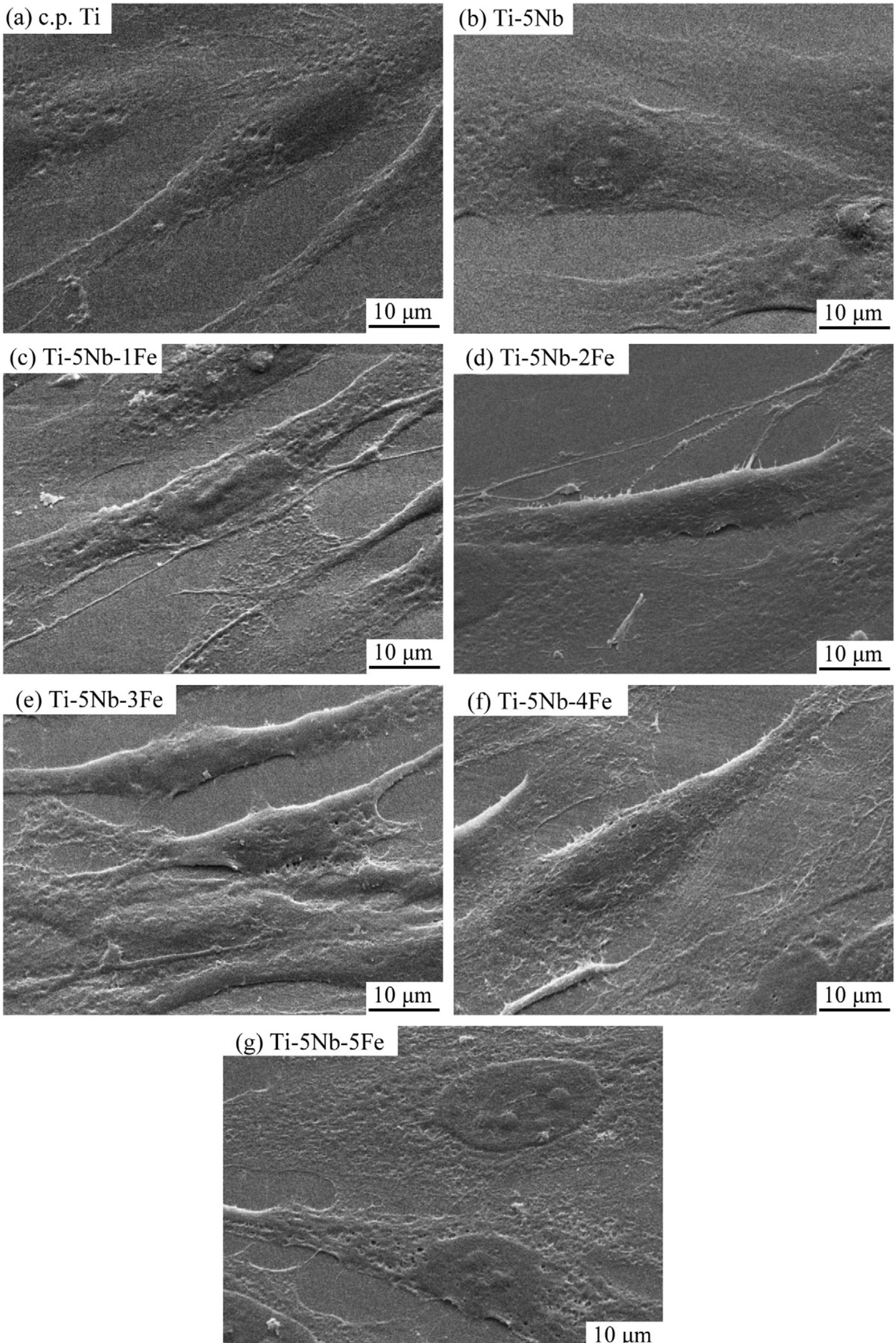

Fig. 8 – SEM micrographs of osteoblastic cells on tested samples after 4 days at 500× magnification.

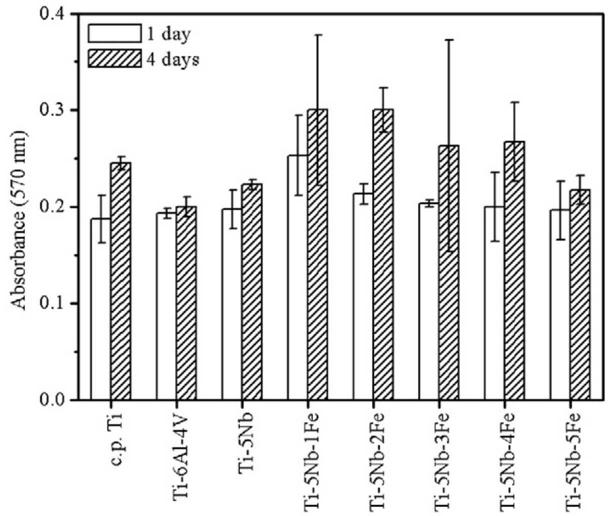

Fig. 9 – Results of the MTT after 1 and 4 days culturing on c.p. Ti, Ti–5Nb and Ti–5Nb–xFe samples.

and Ti–5Nb–5Fe alloys were about 2.5 and 2.9 times greater, respectively, than c.p. Ti.

(3) The Ti–5Nb–3Fe alloy had the highest bending moduli. This result may be associated with the formation of the ω phase during quenching. In contrast, the Ti–5Nb–2Fe alloy had the lowest bending modulus, being lower than that of c.p. Ti by 20%. This alloy exhibited the highest bending strength/modulus ratios of as large as 26.7, which is higher than that of c.p. Ti (8.5) by 214%, and of the Ti–5Nb alloy (14.4) by 85%.

(4) The elastically recoverable angles of the ductile Ti–5Nb–1Fe (19.9°) and Ti–5Nb–5Fe (29.5°) alloys were greater than that of c.p. Ti (2.7°) by as much as 637% and 993%, respectively.

(5) The preliminary cell culturing results revealed that the Ti–5Nb–xFe alloys were not only biocompatible, but supported cell attachment as well.

Acknowledgments

This study was partially supported by grants, NSC 97-2622-E-212-007-CC1 and NSC 98-2622-E-212-001-CC1, which were generously provided by the National Science Council of Taiwan.

REFERENCES

[1] Niinomi M. Recent metallic materials for biomedical applications. Metall Mater Trans A 2002;33:477–86.
[2] Lautenschlager EP, Monaghan P. Titanium and titanium alloys as dental materials. Int Dent J 1993;43:245–53.
[3] Nakajima H, Okabe T. Titanium in dentistry: development and research in the U.S.A. Dent Mater J 1996;15:77–90.
[4] Wang K. The use and properties of titanium and titanium alloys for medical applications in the USA. Mater Sci Eng A 1996;213:134–7.
[5] Okuno O, Hamanaka H. Application of beta titanium alloys in dentistry. Dent Jpn 1989;26:101–4.
[6] Lee CM, Ju CP, Chern Lin JH. Structure–property relationship of cast Ti–Nb alloys. J Oral Rehabil 2002;29:314–22.
[7] Ramirez AJ, Juhas MC. Microstructural evolution in Ti–6Al–4V friction stir welds. Mater Sci Forum 2003;426–432:2999–3004.
[8] Silva HM, Schneider SG, Moura Neto C. Study of nontoxic aluminum and vanadium-free titanium alloys for biomedical applications. Mater Sci Eng C 2004;24:679–82.
[9] Niinomi M. Mechanical properties of biomedical titanium alloys. Mater Sci Eng A 1998;243:231–6.
[10] Hao YL, Li SJ, Sun SY, Zheng CY, Yang R. Elastic deformation behaviour of Ti–24Nb–4Zr–7.9Sn for biomedical applications. Acta Biomater 2007;3:277–86.
[11] Ho WF, Ju CP, Chern Lin JH. Structure and properties of cast binary Ti–Mo alloys. Biomaterials 1999;20:2115–22.
[12] Ho WF. A comparison of tensile properties and corrosion behavior of cast Ti–7.5Mo with c.p. Ti, Ti–15Mo and Ti–6Al–4V alloys. J Alloys Compd 2008;464:580–3.
[13] Ho WF, Chiang TY, Wu SC, Hsu HC. Mechanical properties and deformation behavior of cast binary Ti–Cr alloys. J Alloy Compd 2009;468:533–8.
[14] Ho WF, Chen WK, Wu SC, Hsu HC. Structure, mechanical properties, and grindability of dental Ti–Zr alloys. J Mater Sci Mater Med 2008;19:3179–86.
[15] Hon YH, Wang JY, Pan YN. Composition/phase structure and properties of titanium–niobium alloys. Mater Trans 2003;44:2384–90.
[16] Azevedo CRF, Hippert Jr E. Failure analysis of surgical implants in Brazil. Eng Fail Anal 2002;9:621–33.
[17] Cheal E, Spector M, Hayes W. Role of loads and prosthesis material properties on the mechanics of the proximal femur after total hip arthroplasty. J Orthop Res 1992;10:405–22.
[18] Prendergast P, Taylor D. Stress analysis of the proximo-medial femur after total hip replacement. J Biomed Eng 1990;12:379–82.
[19] Bobyn JD, Glassman AH, Gotto H, Krygier JJ, Miller JE, Brooks CE. The effect of stem stiffness on femoral bone resorption after canine porous-coated total hip arthroplasty. Clin Orthop Relat Res 1990;261:196–213.
[20] Bobyn JD, Mortimer ES, Glassman AH, Engh CA, Miller JE, Brooks CE. Producing and avoiding stress shielding. Clin Orthop Relat Res 1992;274:79–96.
[21] Sumner DR, Galante JO. Determinants of stress shielding: design versus materials versus interface. Clin Orthop Relat Res 1992;274:202–12.
[22] Long M, Rack HJ. Titanium alloys in total joint replacement — a materials science perspective. Biomaterials 1998;19:1621–39.
[23] He G, Eckert J, Dai QL, Sui ML, Löser W, Hagiwara M, Ma E. Nanostructured Ti-based multi-component alloys with potential for biomedical applications. Biomaterials 2003;24:5115–20.
[24] Takahashi E, Sakurai T, Watanabe S, Masahashi N, Hanada S. Effect of heat treatment and Sn content on superelasticity in biocompatible TiNbSn alloys. Mater Trans 2002;43:2978–83.
[25] Ozaki T, Matsumoto H, Watanabe S, Hanada S. Beta Ti alloys with low Young's modulus. Mater Trans 2004;45:2776–9.
[26] Kim JI, Kim HY, Inamura T, Hosoda H, Miyazaki S. Shape memory characteristics of Ti–22Nb–(2–8)Zr(at.%) biomedical alloys. Mater Sci Eng A 2005;403:334–9.
[27] Hosoda H, Miyazaki S. Recent topics of shape memory materials and related technology. J Jpn Soc Mech Eng 2004;107:509–15.
[28] Lee CM, Ho WF, Ju CP, Chern Lin JH. Structure and properties of titanium–25 niobium–x iron alloys. J Mater Sci Mater Med 2002;13:695–700.
[29] Ho WF, Pan CH, Wu SC, Hsu HC. Mechanical properties and deformation behavior of Ti–5Cr–xFe alloys. J Alloy Compd 2009;472:546–50.
[30] Hsu HC, Pan CH, Wu SC, Ho WF. Structure and grindability of cast Ti–5Cr–xFe alloys. J Alloy Compd 2009;474:578–83.
[31] Guha A. Metals Handbook, ninth ed, vol. 8. Ohio: ASM International, Materials Park; 1985.

[32] Hickman BS. The formation of omega phase in titanium and zirconium alloys: a review. J Mater Sci 1969;4:554–63.
[33] Sikka SK, Vohra YK, Chidambaram R. Omega phase in materials. Prog Mater Sci 1982;27:245–310.
[34] Wood RM. Martensitic alpha and omega phases as deformation products in a titanium–15% molybdenum alloy. Acta Metall 1963;11:907–14.
[35] Lyasotskii IV, D'yakonova NB. Structure model for discussion of the peculiarities of the b.c.c.→ω transition in alloys of titanium and zirconium. Phys Met Metallogr 1980;50(1): 118–26.
[36] Afonso CRM, Aleixo GT, Ramirez AJ, Caram R. Influence of cooling rate on microstructure of Ti–Nb alloy for orthopedic implants. Mater Sci Eng C 2007;27:908–13.
[37] Graft WH, Rostoker W. The measurement of elastic modulus of titanium alloys, Symposium on Titanium: Second Pacific Area National Meeting. Philadelphia: ASTM; 1957. pp. 130–144.
[38] Koul MK, Breedis JF. Omega phase embrittlement in aged Ti–V. Metall Trans 1970;1(5):1451–2.
[39] Williams JC, Hickman BS, Marcus HL. The effect of omega phase on the mechanical properties of titanium alloys. Metall Trans 1971;2:1913–9.
[40] Cheng CH, Hsu HC, Wu SC, Wang HW, Ho WF. Effects of chromium addition on structure and mechanical properties of Ti–10Zr alloy. J Alloy Compd 2009;484:524–8.
[41] Koike M, Itoh M, Okuno O, Kimura K, Takeda O, Okabe TH, Okabe T. Evaluation of Ti–Cr–Cu alloys for dental applications. J Mater Eng Perform 2005;14:778–83.